Newton, D., Klee, C., Woodgett, J., & Cohen, P. (1985) *Biochim. Biophys. Acta 845*, 533.
Schreiber, W. E., Sasagawa, T., Titani, K., Wade, R. D., Malencik, D., & Fischer, E. H. (1981) *Biochemistry 20*, 5239.
Small, E. W., & Anderson, S. R. (1987) *Biophys. J. 51*, 555a.
Small, E. W., & Anderson, S. R. (1988) *Biochemistry 27*, 419.
Sobieszek, A., & Barylko, B. (1984) in *Smooth Muscle Contraction* (Stephens, N. L., Ed.) p 283, Dekker, New York.
Steiner, R. F., Marshall, L., & Needleman, D. (1986) *Arch. Biochem. Biophys. 246*, 296.
Wall, C. M., Grand, R. J. A., & Perry, S. V. (1981) *Biochem. J. 193*, 307.
Watterson, D. M., Sharief, F., & Vanaman, T. C. (1980) *J. Biol. Chem. 255*, 962.
Weber, G. (1966) in *Fluorescence and Phosphorescence Analysis* (Hercules, D., Ed.) p 499, Interscience, New York.
Weiss, B., Prozialeck, W., Cimino, M., Sellinger Barnette, M., & Wallace, T. L. (1980) *Ann. N.Y. Acad. Sci. 356*, 319.

Differential Scanning Calorimetry of Cu,Zn-Superoxide Dismutase, the Apoprotein, and Its Zinc-Substituted Derivatives†

James A. Roe, Alison Butler, Diane M. Scholler, and Joan Selverstone Valentine*
Department of Chemistry and Biochemistry and The Molecular Biology Institute, University of California, Los Angeles, Los Angeles, California 90024
Luis Marky and Kenneth J. Breslauer*
Department of Chemistry, Rutgers, The State University of New Jersey, New Brunswick, New Jersey 08903
Received July 14, 1987; Revised Manuscript Received September 18, 1987

ABSTRACT: We have employed differential scanning calorimetry (DSC) to investigate the thermally induced unfolding of native Cu,Zn-superoxide dismutase (SOD), the apoprotein derived from native SOD, and the zinc-substituted derivatives of the apoprotein. We observe two overlapping melting transitions for native bovine SOD with heat capacity maxima at temperatures (T_m) of 89 and 96 °C when a scanning rate of 0.82 deg/min is employed. By contrast, the dithionite-reduced native SOD (which contains Cu^+ rather than Cu^{2+}) exhibits only a single transition at 96 °C. Significantly, we find that the concentration of O_2 present in native SOD samples influences the relative magnitudes of the 89 and 96 °C peaks. Specifically, the lower temperature transition becomes less pronounced as the concentration of O_2 in the sample decreases. On the basis of these observations, we propose that the lower temperature peak corresponds to the melting of the oxidized native protein, while the higher temperature peak reflects the melting of the reduced native protein, which forms spontaneously during the heating process. Our interpretation profoundly differs from that of Lepock et al. [Lepock, J. R., Arnold, L. D., Torrie, B. H., Andrews, B., & Kruuv, J. (1985) *Arch. Biochem. Biophys. 241*, 243–251], who have proposed that the low-temperature transition corresponds to the reduced form of the protein. We present evidence that suggests that their experiments were complicated by the presence of potassium ferrocyanide, which, in addition to reducing the cupric center, also perturbs the protein. In contrast to native SOD, we observe that apo-SOD melts monophasically with a T_m of only 57 °C at the identical scan rate used for melting the native protein. This result demonstrates that metal ions play a significant role in enhancing the thermal stability of native SOD. A series of DSC melts on apo-SOD as a function of added Zn^{2+} reveals that binding of the first 2 equiv of Zn^{2+} ions induces most of the overall thermal stabilization observed for the binding of a total of four Zn^{2+} ions to the SOD protein dimer. While not altering the peak area, addition of the third and fourth equivalents of Zn^{2+} does cause the melting transition to sharpen and to exhibit a small increase in T_m. We also find that the DSC melting profiles for SOD exhibit a strong dependence on scan rate. Such a scan rate dependence can occur when the overall process is kinetically limited and/or irreversible. Consequently, we have considered these possibilities in our interpretation of the calorimetric data.

Native bovine copper–zinc superoxide dismutase (Cu^{II}_2-Zn_2SOD)[1] is a dimer of identical subunits, each of which contains one Cu^{2+} and one Zn^{2+} ion and has an approximate M_r of 16000 (Valentine et al., 1981). The X-ray crystal structure at 2-Å resolution (Tainer et al., 1982) shows a globular protein with each subunit comprised of eight antiparallel β-strands, one disulfide linkage, and a metal binding region in which the Cu^{2+} and Zn^{2+} ions are bridged by a histidyl imidazolate which holds them 6.3 Å apart. In addition to the bridging histidyl imidazolate, the Cu^{2+} ion is coordinated to three histidyl ligands and a water molecule while the Zn^{2+} ion is coordinated to an aspartyl carboxylate group and two histidyl imidazoles (Figure 1). The subunits are strongly

† Supported by USPHS Grants GM-28222 (J.S.V.) and GM-23509 and GM-34469 (K.J.B.).

[1] Abbreviations: Cu,Zn-SOD, native form of cuprozinc superoxide dismutase as isolated from bovine liver. In general, X_2Y_2SOD signifies those derivatives of the native protein in which the metal ions X and Y have been substituted for Cu^{II} and Zn^{II}, respectively (X and Y may be the same). All metal ion oxidation states are assumed to be 2+ unless noted otherwise. E_2Zn_2SOD denotes that protein derivative which is free of metal ions in the copper sites (E = empty).

0006-2960/88/0427-0950$01.50/0 © 1988 American Chemical Society

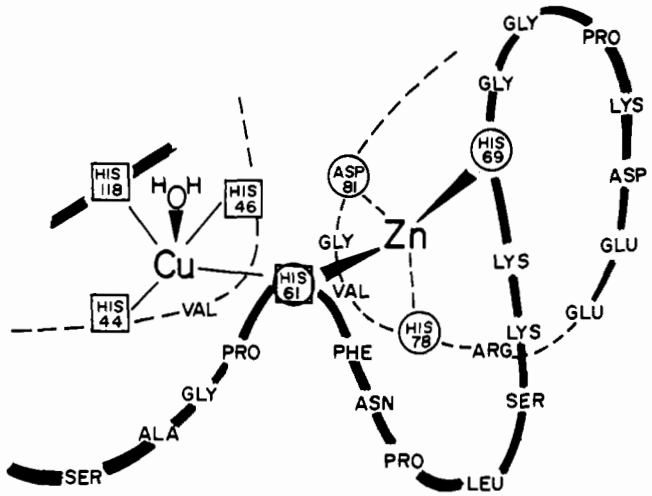

FIGURE 1: Schematic representation of the metal binding region of Cu,Zn-SOD.

associated by noncovalent interactions between residues that occur in a predominantly hydrophobic region of each subunit.[2]

The primary biological function of the superoxide dismutases remains the subject of some controversy (Fridovich, 1981; Fee, 1981). In addition, it is not at all clear what role the zinc ion plays in the native protein, since its removal has little effect on SOD activity (Pantoliano et al., 1982a). NMR experiments, however, have shown that the presence of Zn^{2+} ion influences the structure of the metal binding region of the protein (Cass et al., 1979; Lippard et al., 1977). It has been demonstrated that addition of 2 equiv of Zn^{2+} ion per protein dimer (i.e., one *per subunit*) to the apoprotein causes the conformation of the metal binding region to change to one closely resembling that of the reduced native protein. We have been interested in determining the effect of metal ion binding not only on the local conformation of the metal binding region of the protein but also on the global thermal stability of the entire protein structure.

The work of Forman and Fridovich (1973) and others (Stellwagen & Wilgus, 1978; Simonyan & Nalbandyan, 1975) demonstrates that the protein exhibits a high thermal stability that is large and very sensitive to metal content. For example, Forman and Fridovich found that heating of the apoprotein at 49.4 °C and pH 7.8 for 10 min followed by reconstitution with Cu^{2+} and Zn^{2+} causes 50% of the original activity to be lost. By contrast, the native protein under identical conditions requires heating at 77.2 °C for 10 min to cause loss of half of its activity. The zinc-only derivative was reported to be even less stable than the metal-free form. More recently, Lepock et al. (1985) used differential scanning calorimetry (DSC), to reexamine the thermal stability of the bovine protein as a function of metal content. They concluded, in agreement with Forman and Fridovich, that the native form is thermally more stable than the metal-free protein. However, the melting temperature values reported by Lepock et al. for the native protein and apoprotein are significantly higher than those noted by Forman and Fridovich. Lepock et al. also reported that the zinc-only derivative has a thermal stability between those of the native and the apo forms, in contrast to the result of Forman and Fridovich. In addition, Lepock and co-workers observed that the denaturation of the native protein consists of two transitions of different melting temperatures. They assigned the lower temperature transition to that of the denaturation of a reduced form of the native protein, which contains Cu^{+} rather than Cu^{2+}. In this work, we present evidence that indicates that this assignment is wrong. Lepock et al. based their interpretation on the observation that, in the presence of 4 mM potassium ferrocyanide, the denaturation of the holoprotein appears to occur in a single transition and that the melting temperature of this transition is similar to that of the low temperature denaturing form. We believe that their measurements were complicated by the fact potassium ferrocyanide not only reduces the cupric center but also perturbs the protein. The studies of Lepock et al. were further limited by the fact that they conducted their measurements at only one pH and at only one DSC scan rate.

In the work reported here, we have employed a more sensitive scanning calorimeter and have conducted our measurements at several scan rates. As described below, our results allow us to clarify the nature of the thermal denaturation of bovine Cu,Zn-SOD and to quantify the dependence of the melting behavior on metal content, in particular, the effect of zinc binding on the thermal stability of the protein. Significantly, our results are qualitatively and quantitatively different from those of previous investigators.

Materials and Methods

Proteins and Derivatives. Bovine liver Cu,Zn-SOD was obtained from Diagnostic Data, Inc. (Mountain View, CA), as a lyophilized powder. Protein concentrations of native bovine SOD were determined spectrophotometrically, with $\epsilon_{258nm} = 10300\ M^{-1}\ cm^{-1}$. Reduced native bovine liver SOD was prepared in an inert atmosphere chamber by reduction of native SOD with an approximately 10-fold excess of sodium dithionite in 0.1 M sodium acetate buffer, pH 5.5. Excess dithionite was removed by dialysis against three 1.0-L changes of buffer. Reduction by the direct addition of a small excess of dithionite was also employed. The preparation of the apo-SOD has been described previously (Pantoliano et al., 1982b, 1983), and concentrations were determined by the Lowry assay (Lowry et al., 1951) with a solution of native bovine liver SOD of known concentration for the protein standard. The zinc-containing derivatives were prepared by the direct addition of a buffered solution of 1.53 mM $Zn(NO_3)_2$ (pH 5.5, 100 mM acetate) to an identically buffered apo-SOD solution. Yeast Cu,Zn-SOD was obtained from Pharmacia Copenhagen, and equine liver SOD was a generous gift from Dr. Konrad Lerch. Concentrations of these protein samples were also assayed by the Lowry method with bovine SOD as a standard. Zinc concentrations were confirmed with a Perkin-Elmer 603 atomic absorption spectrometer. To study the influence of dioxygen, lyophilized native SOD was dissolved in buffer and then loaded and sealed in the DSC cells under an inert atmosphere, either argon or a mixture of argon (90%) and hydrogen (10%), or under dioxygen.

Reagents. Glacial acetic acid, sodium acetate, dibasic sodium phosphate, monobasic potassium phosphate, potassium ferrohexacyanide, and the disodium salt of ethylenediaminetetraacetic acid (EDTA) were obtained from Mallinckrodt, AR grade, and used without further purification. HEPES buffer [*N*-(2-hydroxyethyl)piperazine-*N*′-2-ethanesulfonic acid] was obtained from Sigma and used as received. Technical-grade sodium hydrosulfite (sodium dithionite, $Na_2S_2O_4$) was used as obtained from Aldrich. The water used for preparing buffers and other solutions was triply deionized in a Barnstead Nanopure water system.

Calorimetry. Calorimetric measurements were made with a Microcal MC-1 differential scanning calorimeter equipped

[2] Attempts by several investigators have failed to produce stable monomers of this protein except under denaturing conditions. See pp 300–305 of Valentine et al. (1981).

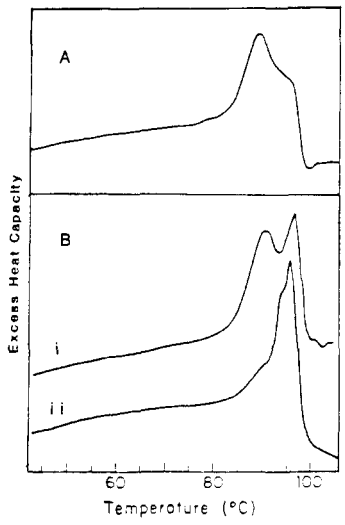

FIGURE 2: DSC scans of native bovine Cu,Zn-SOD and reduced native bovine Cu,Zn-SOD. (A) 0.154 mM native bovine SOD sealed in the DSC cells under a normal atmosphere. (B) (trace i) 0.125 mM SOD sealed in the DSC cells under an inert atmosphere (90% argon and 10% hydrogen); (trace ii) 0.125 mM SOD reduced by dialysis against 50 mM of sodium dithionite and sealed under the same atmosphere as in (i).

with removable hasteloy cells. Each cell was filled to a volume of 0.7 mL. The sample cell contained the protein in buffer solution while the reference cell contained the dialyzate buffer. The temperature was increased from about 15 to 105 °C at various heating rates ranging from 0.19 to 1.62 deg/min. When time-dependent effects were not being investigated, a scan rate of 0.82 deg/min was employed.

Differentical scanning calorimetry (Tsong et al., 1970; Breslauer et al., 1975; Privalov & Potekhin, 1986) provides a temperature-dependent measure of the heat capacity difference between a dilute biopolymer solution and a dialyzate buffer solution. The reference and sample cells are slowly and simultaneously heated at a constant rate while the differential power required to keep the cells at the same temperature is recorded. Endothermic processes are indicated by an increase in the power to sample cell required to keep the two cells at the same temperature. An electrical calibration peak provides the proportionality constant needed to convert differential power to differential heat. The area under a peak, normalized for protein concentration, is proportional to the transition or denaturation enthalpy ΔH_d at the melting temperature T_m. For convenience, we define T_m as the temperature at the peak maximum, although this does not always correspond exactly with 50% completion of a transition. Peak areas were determined with a Gelman Instrument Co. compensating polar planimeter (Model 399231).

Results and Discussion

Native Protein

Figure 2A shows the DSC profile we measured for native bovine $Cu^{II}_2Zn_2SOD$ in 100 mM sodium acetate buffer at pH 5.5. We determined this profile at a scan rate of 0.82 deg/min. Inspection of this DSC profile reveals two partially resolved transitions with maxima at 89 and 96 °C. Although no attempt was made to deconvolute these transitions, we find that the relative intensities of these peaks vary with scan rate. Specifically, with increasing scan rate, the lower temperature peak dramatically increases while the higher temperature endotherm slightly decreases. The net result of these two effects is that the total area under both peaks increases with increasing scan rate. This dependence is illustrated in Figure 3 by a plot of total transition enthalpy versus scan rate. This scan rate dependent behavior is consistent with a model in which the species responsible for the higher temperature endotherm is formed by a relatively slow chemical process or processes from the species responsible for the lower temperature peak. We will elaborate on this model later in the paper.

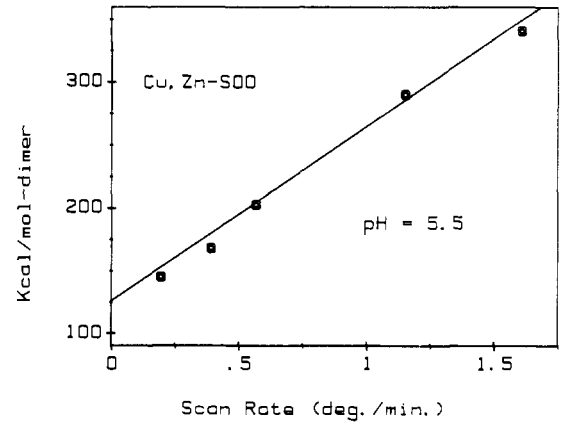

FIGURE 3: Total molar enthalpy of denaturation (includes area beneath both overlapping peaks) for native bovine Cu,Zn-SOD as a function of scan rate. Samples consisted of 0.14 mM native protein in a pH 5.5, 0.1 M acetate buffer.

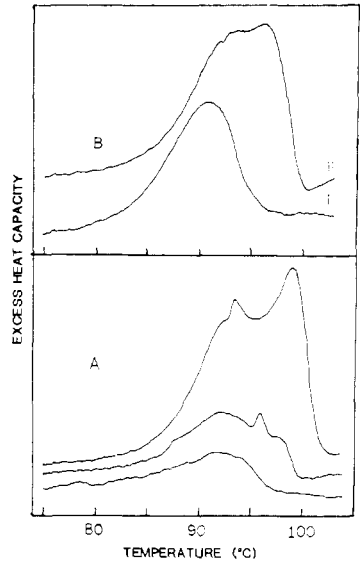

FIGURE 4: (A) Endotherms of native Cu,Zn-SOD at different protein concentrations in a 0.1 M acetate buffer, pH 5.5. The protein concentrations for these samples were 0.35 (top), 0.13 (middle), and 0.02 mM (bottom). Note that the fraction of the scan associated with the higher temperature transition increases with concentration. The gain was increased by a factor of 4 for the bottom trace. (B) DSC scans of native bovine Cu,Zn-SOD in 0.1 M acetate buffer, pH 5.5. Trace i is of 0.10 mM protein in the presence of 4.0 mM $K_4[Fe(CN)_6]$, and trace ii is of 0.35 mM protein in a solution sealed under O_2.

In contrast to the dependence on scan rate, an increase in protein concentration causes an increase in the relative intensity of the peak that corresponds to the thermally more stable form. This behavior is illustrated in Figure 4A by a family of concentration-dependent DSC curves. Significantly, the higher temperature transition exhibits a T_m that is identical with the T_m we measure for the reduced protein, $Cu^{I}_2Zn_2SOD$, prepared by reaction with ascorbate or with dithionite (cf. Figure 2B, trace ii). Taken together, our scan rate dependent and concentration-dependent data suggest that the low-temperature transition corresponds to the native protein, while the high-temperature transition reflects melting of the reduced form of the protein. This reduced form is apparently produced by

the autoreduction of the native protein during the heating process.

To test our interpretation of the biphasic DSC profile of native $Cu^{II}_2Zn_2SOD$, we also conducted a series of calorimetric measurements in which we controlled the amount of dioxygen in the DSC sample by equilibrating identical protein solutions with air, argon, or pure O_2 and sealing them in the DSC cell under each atmosphere. Native SOD dissolved in buffer and sealed in the DSC cell under air exhibited biphasic melting in which the lower temperature transition was predominant (Figure 2A). When sealed under an inert atmosphere (90% Ar, 10% H_2), native SOD again exhibited biphasic melting, but with an increase in the intensity of the higher temperature (96 °C) peak (compare the DSC profile in Figure 2A with curve i in Figure 2B). Saturation of a native SOD sample with dioxygen causes the intensity of the lower temperature (89 °C) peak to increase relative to that observed for an identical sample sealed under air. A DSC scan of a protein sample saturated with O_2 is illustrated in Figure 4B, trace ii (see also Figure 4A, top trace for corresponding air sample). Comparisons between the DSC melting profiles of dithionite-reduced Cu,Zn-SOD, native SOD, and the dioxygen-saturated native sample support our contention that the biphasic melting behavior of native SOD reflects thermally induced reduction of copper with the higher temperature peak corresponding to the reduced form.

As noted in the introduction, our results differ from those of Lepock and co-workers (1985), who concluded that the reduced form of the protein was associated with the low-temperature transition. We attribute this disparity to the fact that they used ferrohexacyanide to reduce the copper center (Viglino et al., 1985). In fact, we have determined that the presence during a DSC scan of either cyanide or ferrohexacyanide in solution with the native protein causes the two transitions to coalesce into a single broad endotherm exhibiting a steadily decreasing melting temperature that is dependent on the concentration of the added ferrocyanide or cyanide (see Figure 4B, trace i). On the basis of this result, we believe that the measurements of Lepock et al. were influenced by an association of ferrohexacyanide or cyanide with the protein rather than resulting from the reduction of the copper center.

Our proposal of the thermally induced reduction of the Cu^{2+} site is consistent with the previous electron paramagnetic resonance (EPR) results of Simonyan and Nalbandyan (1975). These investigators reported that heating bovine erythrocyte Cu,Zn-SOD at 100 °C for 5 min in phosphate buffer at pH 7.2 diminished the copper(II) EPR intensity of the protein. Upon reoxidation, the EPR spectrum of the "regenerated" native SOD differed from that of the "original" native SOD, thereby indicating that the protein environment around the copper had been irreversibly altered.

It is interesting to speculate about the source of the increased thermal stability of reduced SOD, i.e., $Cu^{I}_2Zn_2SOD$, compared to native oxidized SOD, i.e., $Cu^{II}_2Zn_2SOD$. A number of experiments suggest that the imidazolate bridge between the Cu^{2+} and the Zn^{2+} is broken in the reduced protein (Bailey et al., 1980). Such a change might remove a constraint imposed by the configuration of the metal binding region, thereby allowing the overall conformation of the protein to relax to a thermally more stable configuration. However, we recognize that reduction of the cupric site alters not only the initial state but also the final melted state of the protein. When the X-ray crystal structure of the reduced form of the protein becomes available, it will be possible to evaluate more critically the molecular origins of its increased thermal stability.

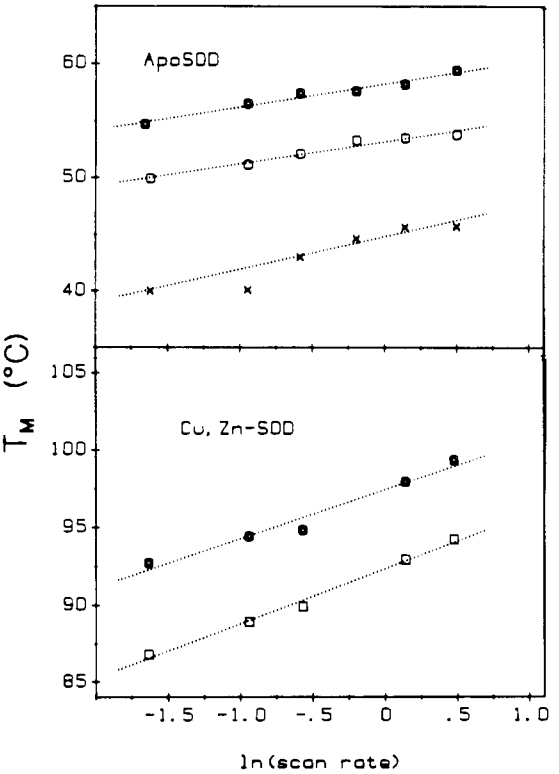

FIGURE 5: (Bottom panel) The observed melting temperatures associated the biphasic melting of native Cu,Zn-SOD as functions of the natural log of the scan rate (deg/min). The protein was dissolved in a 0.1 M acetate buffer, pH 5.5. Open symbols refer to the low-temperature transition, and the solid symbols refer to the higher temperature transition. (Top panel) The observed melting temperature of apo-SOD as a function of the natural log of scan rate (deg/min): (solid symbols) 0.1 M acetate, pH 5.5; (open symbols) 0.1 M HEPES, pH 6.5; (crossed symbols) 0.1 M HEPES, pH 8.0.

Influence of Scan Rate and Protein Concentration on the Observed Melting Temperature. The DSC profiles of native bovine SOD were examined over a 20-fold concentration range, 0.024–0.48 mM. The melting temperatures did not vary with protein concentration. However, as mentioned above, the relative fraction of reduced protein increases with protein concentration. By contrast with the concentration independence of T_m, we find that the T_m's are very sensitive to the scan rate (see the bottom panel of Figure 5). Two possible explanations can be proposed to rationalize this T_m sensitivity to scan rate. (1) The scan rates are too high to allow the denaturing protein to reach equilibrium at each temperature of the DSC scan. Or (2) the denaturation of native SOD is irreversible; that is, the native or initial state cannot be attained again after melting, under the conditions of this study. In connection with the latter possibility, it should be noted that under all conditions employed here rescanning each sample revealed that the native protein denatured irreversibly, even when the scan was stopped halfway through an endotherm.

Under certain conditions, however, irreversible protein denaturations can be thermodynamically interpreted (Privalov & Potekhin, 1986). To analyze thermodynamically the irreversible nature of SOD melting, we follow assumptions similar to those used by Sturtevant and co-workers (Edge et al., 1985). Their approach for thermodynamic analysis of irreversible denaturation is based on a computer simulation of a model protein system that first denatures in a rapid and reversible fashion and then undergoes a slow irreversible step, such as aggregation. The high scan rate sensitivity we observe for the T_m of SOD suggests that the irreversible step in the melting of SOD occurs too rapidly to allow for a simple

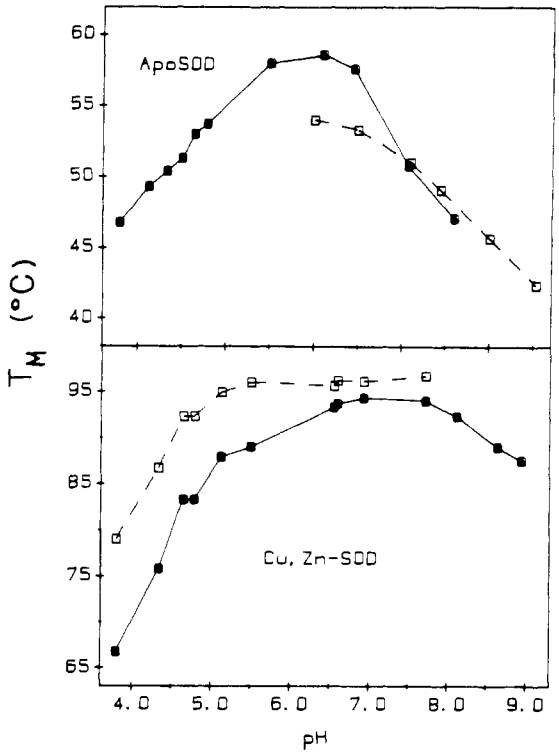

FIGURE 6: (Bottom panel) Melting temperature dependence on pH for Cu,Zn-SOD. The buffer was 0.1 M acetate for pHs <6 and 0.1 M HEPES for pHs ≥6.0. The open and closed symbols refer to the higher and lower temperature peaks, respectively (see text). (Top panel) Melting temperature dependence on pH for apo-SOD: (solid symbols) 0.1 M acetate at pHs <6.0 and 0.1 phosphate at pHs ≥6.0; (open symbols) 0.1 M HEPES.

thermodynamic analysis. In fact, the logarithmic nature of the T_m dependence on scan rate is consistent with a first-order irreversible denaturation (Fujita et al., 1979; Nakamura et al., 1980).

We also observe that the total enthalpy of denaturation increases with the scan rate, as illustrated in Figure 3. Since the melting temperature also increases with the scan rate, the observed enthalpy of denaturation can be said to increase with the melting temperature as well. This increase in the enthalpy may be attributed to the difference in heat capacity (ΔC_p) between the native and denatured forms. However, since we are not able to assign the heat capacity and the enthalpy changes for the irreversible step, it would be inappropriate to attempt a quantitative interpretation of the apparent increase in the enthalpies of denaturation we measure.

Influence of pH. We find the DSC melting profiles of bovine Cu,Zn-SOD to be very sensitive to pH. As shown in the bottom panel of Figure 6, the qualitative characteristics of two overlapping endotherms remain the same at pHs less than 8, but the temperatures of the heat capacity maxima (T_m) vary greatly from lows of 66.8 and 79 °C at pH 3.8 to a plateau which appears from pH 5.0 to pH 8.0. Above pH 8.0, the peaks coalesce to form a single endotherm. If the pH is increased further, the T_m of the single endotherm decreases. As we noted previously, the denaturation of bovine SOD is irreversible throughout the pH range studied. Precipitation accompanies denaturation at pHs between 5.0 and 7.5.

For a reversible transition, the melting temperature of protein denaturation may be dependent on pH if there is a net gain or loss of protons during the transition (Fukada et al., 1983). In such cases, the inverse of the melting temperature will typically show a linear dependence on pH (Calderon et al., 1985). In an irreversible system, where aggregation might be the irreversible process, one might expect a pH dependence in which a T_m minimum is reached near the isoelectric point of the native (or the unfolded) protein. This behavior can be explained as a minimization of intermolecular electrostatic repulsions near the p*I* (Privalov & Potekhin, 1986). However, we observe that the melting temperatures of SOD reach a plateau beginning at pH 5.0. This pH value is very close to Cu,Zn-SOD's isoelectric point of 4.95 (Bannister et al., 1971). This pH dependence of SOD melting is opposite to what would be consistent with aggregation; nonetheless, any pH dependence suggests that electrostatic considerations must be important in the thermal denaturation of SOD.

Native Yeast and Native Equine Liver Cu,Zn-SOD's. We find that native yeast, Cu,Zn-SOD, in 100 mM sodium acetate at pH 5.5, melts at 82 °C with a shoulder at 77 °C. This biphasic melting is similar to the melting behavior we observed for the bovine protein. Significantly, however, the native yeast protein melts at a lower temperature than the corresponding bovine protein. DSC scans of the yeast protein under argon and under O_2 yield results similar to that of bovine SOD. Specifically, the low-temperature transition (77 °C for yeast) increases in intensity under dioxygen while the higher temperature peak at 82 °C increases in intensity under an argon atmosphere. These results suggest that the temperature-dependent reduction we have proposed for native bovine SOD also may occur with the yeast enzyme. Thus, for both native proteins, we propose that the low-temperature transition corresponds to the oxidized protein while the high-temperature transition is due to the denaturation of the reduced form of yeast SOD. However, unlike the behavior we observe for bovine protein, yeast Cu,Zn-SOD does not precipitate after DSC scans at pH 5.5.

Equine liver SOD exhibits quite different melting behavior compared with both bovine and yeast SOD's. Specifically, equine liver SOD melts and precipitates in a single broad transition centered about 93 °C at pH 5.5. Furthermore, this transition is not altered when the protein is sealed under argon or dioxygen atmospheres. The similarity in the melting profiles of the reduced and oxidized forms for equine Cu,Zn-SOD can be explained in either of two ways. The thermal stability of the equine protein, in contrast to that of the bovine or yeast protein, may not depend strongly on the oxidation state of the copper. Alternatively, the thermally induced reduction of the oxidized forms may be completed before the melting temperature is reached. However, the extreme broadness of the equine transition compared with the bovine and yeast transitions makes interpretation difficult.

The similarity in the high degree of thermal stability we observe for bovine SOD (T_m's of 89 and 96 °C) and equine SOD (T_m of 93 °C) is not surprising considering that the amino acid sequences of these proteins show a homology of 80% (Lerch & Ammer, 1981). By contrast, we find that yeast Cu,Zn-SOD, which is only 50% homologous with the bovine protein, denatures at a significantly lower temperature (T_m's of 77 and 82 °C). Our results with yeast Cu,Zn-SOD, as well as those for the bovine protein, are significantly different than those reported by Arnold and Lepock (1982). In particular, they observed a T_m of 88 °C for the yeast enzyme, whereas we measure the reduced yeast SOD transition at 82 °C. This disparity in observed T_m values in part may reflect differences in pH (pH 7.4 vs. pH 5.5) in addition to differences in scan rate. Arnold and Lepock employed a scan rate of 2.5 deg/min. in their study while we used 0.82 deg/min. If the denaturation of the yeast protein is a relatively slow process, an increase in the scan rate would result in an increase of the measured

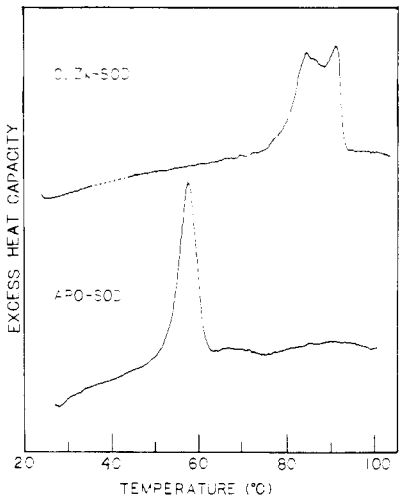

FIGURE 7: DSC traces of native bovine Cu,Zn-SOD (top) and the metal-free protein (apo-SOD) in 0.1 M acetate, pH 5.5.

melting temperature (Fujita et al., 1979). Arnold and Lepock (1982) also observed a second transition at 77 °C which they attributed to a new hybrid dimer. This peak appears only after a cycle of heating beyond the T_m and upon cooling. We also observe two transitions in the initial heating and cooling cycle, but we interpret them as consequences of a different process, i.e., the thermally induced reduction of the yeast SOD.

Apoprotein

Occupancy of the Metal Binding Sites Increases the Thermal Stability of the Apoprotein. Removal of metal ions from bovine Cu,Zn-SOD, to form the apoprotein, dramatically decreases the thermal stability of the protein. Specifically, as illustrated in Figure 7, the thermally induced unfolding of apo-SOD in 100 mM sodium acetate buffer, pH 5.5, occurs as a single transition with a T_m of only 57 °C at the scan rate of 0.82 deg/min. This T_m of only 57 °C for the apoprotein should be compared with a T_m of 89 °C for the oxidized native bovine Cu,Zn-SOD in which the metal binding sites are fully occupied.

Apo-SOD Renatures at pH 3.8. Recall that the native holoprotein irreversibly denatures under all experimental conditions studied. By contrast, the denaturation of the apoprotein at pH 3.8 in 100 mM acetate is partially reversible, even after four scanning cycles. Specifically, when a 0.30 mM solution of apo-SOD is scanned and rescanned from 15 to 60 °C at a rate of 0.82 deg/min under the above conditions, the DSC trace of the fourth scan retains 14% of the area of the initial scan. The percentage of the transition that is reversible appears to be dependent on the concentration of the protein, the scan rate, and the temperature at which the scan is halted. Increases in protein concentration and final scan temperature both independently decrease the percentage of protein that renatures. By contrast, an increase in scan rate causes an increase in the percentage of protein that renatures. For example, when two identical samples are heated to 55 °C at 0.39 and 1.62 deg/min, 44% and 68% renatures, respectively (Figure 8).

Influence of Protein Concentration. We examined the DSC melting profile of apo-SOD at pH 5.5 over a 10-fold concentration range (0.032–0.32 mM protein). The melting temperature and the molar enthalpy of denaturation did not vary with the protein concentration. We conclude from these results that the denaturation step of apo-SOD is first order in protein concentration over the range studied.

Scan Rate Increases the Observed Melting Temperature of Apo-SOD. The top panel of Figure 5 shows plots of T_m

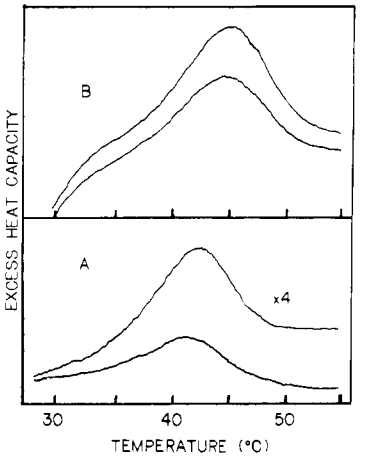

FIGURE 8: DSC traces of two identical 0.27 mM apo-SOD samples in 0.1 M acetate, pH 3.8, at different scan rates. (A) was measured at a rate of 0.39 deg/min and (B) at 1.62 deg/min. The upper curve in each panel is of the initial scan, and the lower curve is of the second scan of each sample.

versus ln (scan rate) of the apoprotein at three pHs. This sensitivity to the scan rate is similar to that which we observe for the native protein. As with the native protein, such a dependence on scan rate suggests either that the overall melting process involves an irreversible step or that the scan rates were too fast to allow proper equilibration of the system at each temperature. In the case of apo-SOD melting at pH 3.8, we have noted that partial reversibility is observed, but the complete renaturation and denaturation processes are too slow for equilibration even at our slowest scan rate of 0.19 deg/min. At the other pHs studied (see the top panel of Figure 5), we find no indication of reversibility. These results suggest that the observed dependence on scan rate is a consequence of a kinetically controlled process.

One possible model for the melting behavior of the metal-free SOD at pH 3.8 involves two steps, a reversible protein unfolding followed by a slower but irreversible process such as aggregation. This scheme, which has been used by others including Edge et al. (1985) to interpret DSC data on irreversible systems, is illustrated as

$$N \underset{}{\overset{\text{fast}}{\rightleftharpoons}} D \xrightarrow{\text{slow}} A$$

where N denotes the native or folded form of the protein, D denotes the denatured form, and A denotes the aggregated form. In this model, the native form of the protein is in a fast equilibrium with the denatured form. During a DSC temperature scan, the relative fraction of protein in the native form decreases as the fraction of the denatured form increases. This denaturation transition corresponds to the first, reversible step of the two-step melting process. If the second, irreversible step is slow (e.g., aggregation), then a significant fraction of the total protein will renature from the unfolded state. When the scan is complete and the sample is cooled, we observe several characteristics of the melting behavior of apo-SOD that are consistent with the scheme for melting noted above: (1) the sample *does* renature to some degree; (2) the fraction of the sample which renatures depends on the rate of scan, the original concentration of the protein, and the temperature at which the scan is halted.

Since we do not observe reversibility for the protein melting under conditions other than pH 3.8 and demetallation, it would be inappropriate for us to interpret the native Cu,Zn-SOD melting behavior in terms of this simple two-step model. In fact, a simple one-step, irreversible process also is consistent with the data we measure for irreversible Cu,Zn-SOD melting.

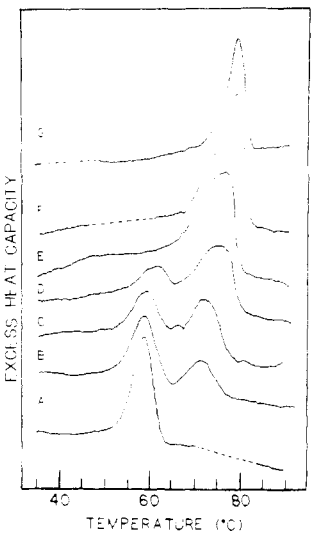

FIGURE 9: DSC scans of apo-SOD with increasing amounts of Zn^{2+} added. The protein concentration was 0.128 mM buffered in 100 mM acetate at pH 5.5. In (A), the sample is apo-SOD with no Zn^{2+} added. In (B–G), 0.5, 1.0, 1.5, 2.1, 3.1, and 4.1 equiv of Zn^{2+} per protein dimer had been added to the apoprotein sample. The gain for (G) had been decreased by a factor of 2. Electrical calibration pulses have been deleted for clarity and replaced by dotted lines.

Influence of pH. As with the native protein, the melting temperature we measure for the apo-SOD transition is very pH sensitive (see the top panel of Figure 6). At a scan rate of 0.82 deg/min, the T_m of the apoprotein reaches a maximum of 58 °C between pH 5.5 and pH 6.0 in acetate buffer. The native protein shows similar behavior by reaching a maximum melting temperature at a pH only about 0.5 unit lower. By contrast with the pH-dependent behavior, the addition of metal ions greatly affects other melting properties of SOD. The similarity in pH dependence between the native and metal-free forms of SOD may suggest similar mechanisms of protein melting. Unfortunately, the isoelectric point of the apoprotein is not known, so that further comparison is difficult. Nevertheless, the similarity in the pH dependence of the melting behavior of both the native and metal-free forms of SOD may reflect a similar electrostatic potential on the surface of the protein. The calculations of Klapper et al. (1986) have indicated that the surface of Cu,Zn-SOD possesses a negatively charged electric field. This negative field on the exterior of the protein may not be perturbed greatly by the demetallation of the native enzyme, since demetallation affects the potential of a fairly small region of the protein, namely, the active site, which is not located on the surface.

Zinc-Substituted Derivatives

Quantifying the Stabilizing Influence of Zn^{2+}. Spectra B–G of Figure 9 show a series of DSC scans on apoprotein solutions to which variable amounts of zinc ion have been added. NMR studies have demonstrated previously that under comparable conditions essentially all the added Zn^{2+} ion (up to 4 equiv per apoprotein dimer) is bound by the protein (Hirose et al., 1984; Cass et al., 1979; Lippard et al., 1977). Several significant features of the results illustrated in Figure 9 should be noted. (1) Addition of 1 equiv of Zn^{2+} per dimer (Figure 9C) causes the apoprotein peak to be diminished by approximately 50% with a new peak appearing at 72 °C. We interpret this result as reflecting a one-to-one mixture of the apoprotein and the two-Zn^{2+} derivative. (2) The disappearance of the apoprotein peak and the full development of the higher temperature peak are complete after addition of two zinc ions per protein dimer (see Figure 9E), i.e., at 1 equiv of zinc per subunit. (3) Successive additions of zinc ion above 2 equiv per protein dimer (Figure 9F,G) causes a gradual change in the shape of the transition (it becomes sharper) and a shift of the T_m from 72 to 79 °C. However, upon the addition of zinc ions beyond 2 equiv, the area beneath the transition curve (ΔH) remains constant (see below). In other words, E_2Zn_2-SOD and Zn_2Zn_2SOD exhibit nearly the same melting behavior when characterized by denaturation enthalpies and melting temperatures. (4) Addition of more than 4 equiv of Zn^{2+} has little or no effect on the DSC profile. This observation suggests that nonspecific binding of zinc to the protein, if it does occur under these conditions, does not further increase the thermal stability of Zn_2Zn_2SOD or otherwise influence its melting behavior.

The results listed above are consistent with an interpretation in which the binding of the first 2 equiv of Zn^{2+} to the metal sites of the dimer are not statistical. Instead, a two-Zn^{2+} dimer is preferentially formed in a cooperative manner between the subunits. (Presumably E_2Zn_2SOD represents this two-Zn^{2+} dimer where one zinc ion is bound at the zinc site of each of the two subunits.) If zinc binding to the zinc sites were not cooperative, then we would expect to observe three DSC transitions during the Zn^{2+} titration of SOD. These theoretical transitions would correspond to the apoprotein and the one-zinc and the two-zinc derivatives. Obviously, this expectation assumes that the three transitions can be resolved.

The denaturations of the apo and zinc-substituted forms of SOD under the conditions of the zinc titration are irreversible. Consequently, our thermodynamic interpretation of the zinc binding equilibria should be viewed with caution. In fact, an alternative denaturation mechanism also is consistent with our results. This mechanism requires the apo-SOD and zinc derivatives to denature as well as individual subunits. However, totally independent denaturation of both subunits requires either that the unfolding of one subunit has no effect on the remaining associated unit or that the protein monomerizes prior to denaturation. The former assumption is highly unlikely because the two subunits are associated by strong hydrophobic interactions. Consequently, one would expect that the denaturation of one subunit would dramatically affect the structure of the second. Monomerization of the protein under these conditions also is unlikely considering studies which have demonstrated the strength of subunit association (Valentine et al., 1981).

Zn^{2+} Binding Increases the Denaturation Enthalpy. The overall transition enthalpies obtained from the areas under the apoprotein peak and the higher temperature peak (i.e., the zinc derivatives) are plotted in Figure 10 as a function of added zinc ion. These representations of the data illustrate two important points: (1) the apoprotein has all but disappeared after addition of only 2 equiv of zinc per dimer, and (2) the large metal-induced increase in denaturation enthalpy is complete after addition of only 2 equiv of zinc per dimer. These results further support our conclusion that a two-zinc dimer is formed rather than a collection of dimers containing zinc distributed in a statistical fashion between the two zinc sites. Moreover, the ΔH_d is nearly constant at ratios of zinc-to-dimer greater than 2, as reflected by the plateau region in Figure 10. This result suggests that two zinc ions are sufficient to induce nearly all of the stabilization provided by binding up to four zinc ions. In fact, under one set of identical conditions SOD derivatives which have two or more equivalents of bound zinc have melting enthalpies (ΔH_d) identical within experimental error to that of native Cu,Zn-SOD. Specifically, when the DSC scans are carried out at a scan rate of 0.82

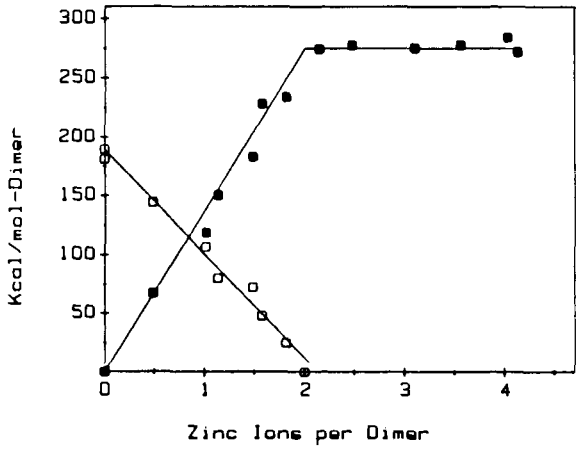

FIGURE 10: Plots of the normalized transition enthalpies (ΔH_d, kcal mol^{-1} dimer^{-1}) calculated for the apo-SOD endotherm as it disappeared (open symbols) and for the high-temperature (72–79 °C) peak as it increased (solid symbols) as functions of added Zn^{2+}. The total protein concentration varied from 0.125 to 0.128 mM and was buffered in 100 mM acetate at pH 5.5.

deg/min and a pH of 5.5 in 100 mM acetate buffer, and with a protein concentration near 0.15 mM, the zinc derivatives, which have two or more bound equivalents, exhibit ΔH_d's of 279 ± 13 kcal/mol (an average of six trials) as compared to the ΔH_d of 280 ± 15 kcal/mol (an average of five trials) measured from scans of the native fully metallated protein, Cu,Zn-SOD.

We also have employed titration calorimetry (both isothermal and isoperibol) to monitor the binding of zinc ions by apo-SOD. These studies reveal that the binding of the first two zinc ions per protein dimer is a strongly exothermic process. We observed no further heat effect upon the addition of the third and fourth equivalents of Zn^{2+} (unpublished data). These titration calorimetric results are consistent with the DSC data shown in Figure 10, which demonstrate that only the first 2 equiv of added Zn^{2+} contribute significantly to the enthalpic stabilization.

Cass et al. (1979) and Lippard et al. (1977) have reported that the NMR spectrum of apo-SOD after addition of 1 equiv of Zn^{2+} per protein dimer is a superposition of the spectrum of apo-SOD and that of the two-zinc derivative. These investigators interpret their results as indicating that the metal binding region of an apoprotein subunit is not substantially affected when zinc is bound to the other subunit. However, their results also are consistent with cooperative binding of the first two zinc ions by SOD. Either interpretation adequately explains the NMR data. The NMR work of Lippard and co-workers also showed that all 4 equiv of zinc added to the protein solution affect the NMR of SOD, thereby suggesting that all the zinc is bound at the active site. On the basis of this NMR study, we have assumed a model in which the first 4 equiv of zinc bind to the metal binding region, rather than a model in which two zinc ions bind tightly at the metal binding region while the remaining two zincs associated with some other region of the protein. However, it should be noted that the NMR study was carried out in phosphate buffer, whereas this calorimetric study was conducted in acetate buffer.

Comparison with DSC Studies on Alkaline Phosphatase. It is of interest to compare our results with previously published DSC studies on alkaline phosphatase (AP) (Chlebowski & Mabrey, 1977; Chlebowski et al., 1979). Like SOD, AP also is a dimeric protein containing multiple metal ion binding sites. The apo-AP dimer melts at 57.5 °C while the native protein is thermally more stable, melting in a biphasic process with melting transitions at 89.8 and 90.0 °C, when a scanning rate of 1 deg/min is employed. A zinc titration of the apoenzyme monitored by DSC shows only two discrete transitions corresponding to apo-AP and Zn_2-AP. A plot of the decrease in ΔH_d for apo-AP or the increase in ΔH_d for zinc-bound AP versus the equivalents of Zn^{2+} ions added per dimer is linear and breaks at two Zn^{2+} per dimer. This result suggests that Zn^{2+} binds to apo-AP in a cooperative manner. Successive additions of either Zn^{2+} or Mn^{2+} increase the T_m values slightly (~5 °C) and also increse the enthalpies of denaturation slightly. These results closely parallel our own work on SOD and suggest a general role for the influence of certain metal ions on the thermal stability and melting behavior of biomolecules.

Nature of Transitions

We have calculated van't Hoff enthalpies from the SOD melting curves using the expression (Privalov, 1979)

$$\Delta H_{vH} = 4RT_m^2(\Delta C_{p(max)}/\Delta H_d)$$

This calculation assumes a two-state, reversible transition. The resulting model-dependent van't Hoff enthalpies can be compared with the model-independent calorimetric enthalpies (ΔH_d) by using the ratio $\Delta H_d/\Delta H_{vH}$. If a transition occurs in a single step, this ratio is unity (i.e., the van't Hoff and the calorimetric denaturation enthalpies are equal). For the partially reversible denaturation of apo-SOD at pH 3.8, this ratio is 1.1 (an average of five trials). This value implies that under these conditions the denaturation of the entire SOD dimer is a cooperative process that approaches two-state behavior. However, this analysis is only strictly appropriate for reversible denaturations. Sturtevant and co-workers have shown that this thermodynamic formulation can be applied to irreversible cases, when certain assumptions are made (Edge et al., 1985). Following their treatment, we have analyzed the melting profiles of the four-zinc derivative, the reduced native form, and the apoprotein at pH 5.5. All three forms exhibit $\Delta H_d/\Delta H_{vH}$ ratios of 1.3. As in the partially reversible case, these ratios suggest that a significant fraction of these three forms of the protein denatures in a concerted fashion. However, because of the irreversible nature of these protein systems, the calorimetric data must be viewed with caution. We have not conducted a similar treatment on the DSC profiles of the native (oxidized) form because of the presence of the second overlapping endotherm. In this work, we have not attempted to deconvolute these overlapping heat capacity curves.

CONCLUSIONS

The results we have presented here indicate that the general melting behavior and the thermal stability of SOD are very sensitive to the degree of demetallation and pH. The scan rate dependence of the DSC endotherms and the irreversible nature of SOD denaturation (except for the yeast protein and the demetallated bovine protein at pH 3.8) require that the melting behavior of SOD be analyzed by models which account for potential kinetic (e.g., slow aggregation) as well as thermodynamic influences.

Significantly, we also have shown that the biphasic nature of native SOD reflects the thermally induced reduction of the cupric center, with the higher temperature transition corresponding to the melting of the reduced species. We have quantified the zinc ion induced thermal stabilization of the protein at pH 5.5 and have shown that most of this stabilization results from the binding of the first 2 equiv of Zn^{2+} by the

protein. In addition, we have shown that the melting behavior of the zinc derivatives is consistent with cooperative or pairwise binding of the first 2 equiv of zinc. This last conclusion should be viewed as tentative, since the denaturation of the zinc derivatives is not reversible.

Registry No. Cu,Zn-SOD, 9054-89-1.

REFERENCES

Arnold, L. D., & Lepock, J. R. (1982) *FEBS Lett. 146*, 302–305.

Bailey, D. B., Ellis, P. D., & Fee, J. A. (1980) *Biochemistry 19*, 591–596.

Bannister, J., Bannister, W., & Wood, E. (1971) *Eur. J. Biochem. 18*, 178–186.

Breslauer, K. J., Sturtevant, J. M., & Tinoco, I., Jr. (1975) *J. Mol. Biol. 99*, 549–565.

Calderon, R. O., Stolowich, N. J., Gerlt, J. A., & Sturtevant, J. M. (1985) *Biochemistry 24*, 6044–6049.

Cass, A. E. G., Hill, H. A. O., Bannister, J. V., & Bannister, W. H. (1979) *Biochem. J. 177*, 477–486.

Chlebowski, J. F., & Mabrey, S. (1977) *J. Biol. Chem. 252*, 7042–7052.

Chlebowski, J. F., Mabrey, S., & Falk, M. M. (1979) *J. Biol. Chem. 254*, 5745–5753.

Edge, V., Allewell, N. M., & Sturtevant, J. M. (1985) *Biochemistry 24*, 5899–5906.

Fee, J. A. (1981) in *Oxygen and Oxy-Radicals in Chemistry and Biology* (Rodgers, M. A. J., & Powers, E. L., Eds.) pp 205–239, Academic, New York.

Forman, H. J., & Fridovich, I. (1973) *J. Biol. Chem. 248*, 2645–2649.

Fridovich, I. (1981) in *Oxygen and Oxy-Radicals in Chemistry and Biology* (Rodgers, M. A. J., & Powers, E. L., Eds.) pp 197–204, Academic, New York.

Fujita, S. C., Go, N., & Imahori, K. (1979) *Biochemistry 18*, 24–28.

Fukada, H., Sturtevant, J. M., & Quiocho, F. A. (1983) *J. Biol. Chem. 258*, 13193–13198.

Hirose, J., Yamada, M., Hayakawa, C., Nagao, H., Noji, M., & Kidani, Y. (1984) *Biochem. Int. 8*, 401–408.

Klapper, I., Hagstrom, R., Fine, R., Sharp, K., & Honig, B. (1986) *Proteins 1*, 47–59.

Lepock, J. R., Arnold, L. D., Torrie, B. H., Andrews, B., & Kruuv, J. (1985) *Arch. Biochem. Biophys. 241*, 243–251.

Lerch, K., & Ammer, D. (1981) *J. Biol. Chem. 256*, 11545–11551.

Lippard, S. J., Burger, A. R., Ugurbil, K., Pantoliano, M. W., & Valentine, J. S. (1977) *Biochemistry 16*, 1136–1141.

Lowry, O. H., Rosebrough, N. J., Farr, A. L., & Randall, R. J. (1951) *J. Biol. Chem. 193*, 265–275.

Nakamura, S., Koga, K., & Yoshizumi, H. (1980) in *Proceedings of The Sixth International Symposium on Flavins and Flavoproteins* (Yagi, K., & Yamano, T., Eds.) pp 107–115, University Park Press, Baltimore, MD.

Pantoliano, M. W., Valentine, J. S., Burger, A. R., & Lippard, S. J. (1982a) *Inorg. Biochem. 17*, 325–341.

Pantoliano, M. W., Valentine, J. S., & Nafie, L. A. (1982b) *J. Am. Chem. Soc. 104*, 6310–6317.

Pantoliano, M. W., Valentine, J. S., Mammone, R. J., & Scholler, D. M. (1983) *J. Am. Chem. Soc. 104*, 1717–1723.

Privalov, P. L. (1979) *Adv. Protein Chem. 33*, 167–241.

Privalov, P. L., & Potekhin, S. A. (1986) *Methods Enzymol. 131*, 4–51.

Simonyan, M. A., & Nalbandyan, R. M. (1975) *Biokhimiya (Moscow) 40*, 726–732 [*Biochemistry (Engl. Transl.) 40*, 616–622].

Stellwagen, E., & Wilgus, H. (1978) in *Biochemistry of Thermophily* (Friedman, S. M., Ed.) pp 223–232, Academic, New York.

Tainer, J. A., Getzoff, E. D., Beem, K. M., Richardson, J. S., & Richardson, D. C. (1982) *J. Mol. Biol. 160*, 181–217.

Tsong, T. Y., Hearn, R. P., Wrathall, D. P., & Sturtevant, J. M. (1970) *Biochemistry 9*, 2666–2677.

Valentine, J. S., & Pantoliano, M. W. (1981) in *Copper Proteins* (Spiro, T. G., Ed.) pp 291–358, Wiley, New York.

Viglino, P., Scarpa, M., Cocco, D., & Rigo, A. (1985) *Biochem. J. 229*, 87–90.